International Journal of Modern Physics A

Elliptic flow of light nuclei in Au+Au collisions at $\sqrt{s_{NN}} = 14.6, 19.6, 27$, and 54.4 GeV using the STAR detector

Rishabh Shamra (for the STAR Collaboration)

Indian Institute of Science Education and Research (IISER)
Tirupati, A.P. - 517507, India
rishabhsharma@students.iisertirupati.ac.in

The production of light nuclei in relativistic heavy-ion collisions is usually described by the thermal model and the coalescence model. The thermal model suggests that the light nuclei are emitted by a source in local thermal equilibrium with other hadrons and their yields are fixed at chemical freeze-out. However, given that the binding energies of light nuclei are only of the order of a few MeV, it is more likely that they are formed at a later stage by the coalescence of protons and neutrons near the kinetic freeze-out surface. The final-state coalescence of nucleons can lead to the mass number scaling of the elliptic flow of light nuclei. This scaling states that the elliptic flow of light nuclei scaled by their respective mass numbers will follow very closely the elliptic flow of nucleons. Therefore, studying the elliptic flow of light nuclei will help us in understanding their production mechanism.

In these proceedings, we report transverse momentum (p_T) and centrality dependence of elliptic flow (v_2) of d, t, and ^{3}He in Au+Au collisions at $\sqrt{s_{NN}} = 14.6$, 19.6, 27, and 54.4 GeV from the second phase of the Beam Energy Scan program by the STAR Collaboration. In addition, mass number scaling of $v_2(p_T)$ of light nuclei is discussed.

Keywords: elliptic flow, light nuclei, heavy-ion collisions

PACS numbers:

1. Introduction

The production of light nuclei in relativistic heavy-ion collisions has been a topic of interest in both theoretical and experimental studies.[1] Although, light nuclei are produced in abundance in heavy-ion collisions, their production mechanism still remains to be understood. There are various models[2] that try to explain the production mechanism, however, two main models are the thermal model and the coalescence model. The thermal model[3] suggests that light nuclei are produced at chemical freeze-out (CFO) surface in chemical equilibrium with the rest of the hadrons. However, given the small binding energies (∼MeV) of light nuclei it is not very clear how they might be able to survive the high temperature at the CFO.

The coalescence model,[4] on the other hand, suggests that light nuclei are formed by the final-state recombination of protons and neutrons that are close to each other in phase space at later stages of the collision. Unlike quark coalescence, in case of nucleon coalescence the momentum space information of both the constituents (nucleons) and product (nuclei) are available. One of the consequences expected from the production via coalescence model is the mass number scaling[5] of elliptic flow. If coalescence picture is correct, it is expected that elliptic flow of light nuclei scaled by their respective mass numbers will be close to the elliptic flow of protons. Therefore, studying the elliptic flow of light nuclei in heavy-ion collisions can help in understanding of their production mechanism.

2. Analysis details

The data presented in these proceedings is from the second phase of beam energy scan (BES-II) program collected by the STAR Experiment at RHIC. We report results from Au+Au collisions at $\sqrt{s_{NN}} = 14.6$, 19.6, 27, and 54.4 GeV collected in the period of 2017-2019.

Light nuclei identification is performed using the Time Projection Chamber (TPC)[6] and the Time of Flight (TOF)[7] detector . The TPC is the primary tracking device in the STAR experiment which uses specific ionisation energy loss (dE/dx) in a large gas volume to detect trajectories of charged particles. The curvature of the tracks of particles allows to determine their charge sign and rigidity (momentum/charge). In 2019, the inner TPC sectors were upgraded (iTPC) by increasing the segmentation of the inner padplane from 13 to 40 and renewing the inner sector wires.[8] The revamped iTPC provides increased pseudorapidity (η) coverage from $|\eta| < 1.0$ to $|\eta| < 1.5$, better momentum resolution, and better dE/dx resolution. Figure 1(a) is a representative plot of measured $\langle dE/dx \rangle$ versus rigidity for minimum bias Au+Au collisions at $\sqrt{s_{NN}} = 54.4$ GeV. The theoretical curves calculated from Bichsel function[9] are shown as solid lines.

The TOF detector at STAR uses multigap resistive plate chambers (MRPCs). The TOF detector and the vertex position detector (VPD)[10] measure the time interval (t) over which a particle travels from the primary collision vertex to a read-out cell of the TOF detector. This time-interval information is combined with the total path (S) length measured by the TPC to provide the inverse velocity, $1/\beta = ct/S$, where c is the speed of light. TOF detector enables the light nuclei identification by imposing a constraint on their mass-over-charge-square given by $m^2/q^2 = p^2(1/\beta^2 - 1)$. Figure 1(b) shows m^2/q^2 as a function of the particle momentum for minimum-bias Au+Au collisions at $\sqrt{s_{NN}} = 14.6$ GeV. The horizontal lines depict the expected m^2/q^2 of various light nuclei.

The angular distribution of all the reconstructed charged particles with respect to the symmetry planes (Ψ_n) can be expanded into a Fourier series[11]

$$E\frac{d^3N}{dp^3} = \frac{1}{2\pi}\frac{d^2N}{p_T dp_T dy}\left(1 + \sum_{n=1}^{\infty} 2v_n \cos[n(\phi - \Psi_n)]\right), \tag{1}$$

where E, p, and ϕ are the energy, momentum, and azimuthal angle of the particle, respectively. Fourier coefficients v_n can be estimated using

$$v_n = \langle \cos(n(\phi - \Psi_n)) \rangle. \tag{2}$$

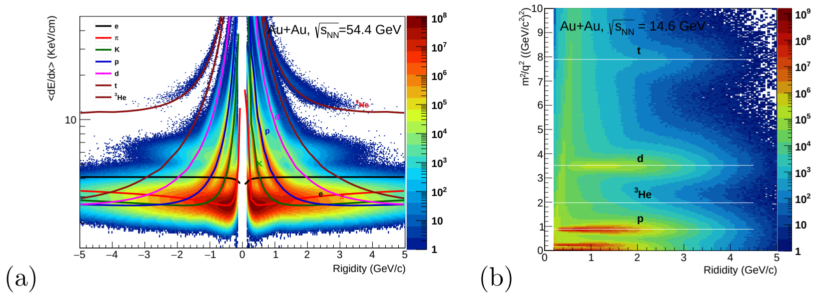

Fig. 1. (a) Specific ionisation energy loss ($\langle dE/dx \rangle$) as a function of rigidity measured by TPC in minimum bias Au+Au collisions at $\sqrt{s_{NN}} = 54.4$ GeV. Solid lines are predictions from Bichsel function. (b) Mass-over-charge-square as a function of rigidity measured by TOF in minimum bias Au+Au collisions at $\sqrt{s_{NN}} = 14.6$ GeV. Solid lines correspond to the m^2/q^2 of various light nuclei.

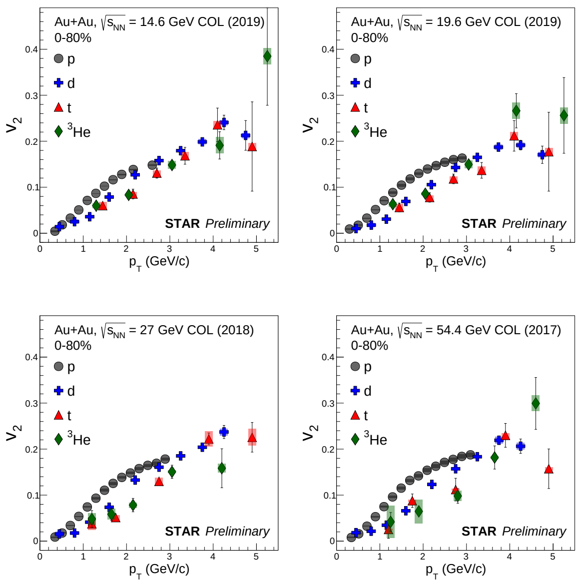

Fig. 2. $v_2(p_T)$ p, d, t, and ^{3}He in minimum bias Au+Au collisions at $\sqrt{s_{NN}} = 14.6$, 19.6, 27, and 54.4 GeV. Vertical lines and shaded area at each marker represent statistical and systematic uncertainties, respectively.

The second order coefficient of the Fourier series (v_2) is called elliptic flow and is related to the initial geometrical anisotropy of the overlap region of the colliding nuclei. v_2 of light nuclei has been measured using second order event plane angle (Ψ_2) estimated from the tracks reconstructed in the TPC[6] for Au+Au collisions at $\sqrt{s_{NN}} = 27$ and 54.4 GeV and the TPC and iTPC[8] for Au+Au collisions at

$\sqrt{s_{NN}}$ = 14.6 and 19.6 GeV. The η-subevent plane method is used to reduce auto-correlation.[12] This method involves dividing each event into two separate subevents based on η windows: $0.05 < |\eta| < 1.0$ (1.5 for iTPC). Within each subevent, v_2 is calculated using the Ψ_2 from the opposite subevent. This η gap of 0.1 between the subevents reduces short-range correlations.

3. Elliptic flow of light nuclei

Figure 2 shows v_2 of p, d, t, and ^{3}He as a function of transverse momentum (p_T) in 0-80% centrality interval in Au+Au collisions at $\sqrt{s_{NN}}$ = 14.6, 19.6, 27, and 54.4 GeV. A monotonous increase of v_2 of light nuclei with p_T is observed across all four center-of-mass energies. We also observe a mass ordering at low p_T between $1-2$ GeV/c.

4. Centrality dependence of elliptic flow

Figure 3 shows the centrality dependence of v_2 of d measured in two centrality ranges, 0-30% and 30-80%, in Au+Au collisions at $\sqrt{s_{NN}}$ = 19.6, 27, and 54.4 GeV. It is observed that peripheral collisions have a higher v_2 of d compared to central collisions. This observation is a consequence of larger spatial anisotropy in peripheral collisions compared to central collisions.

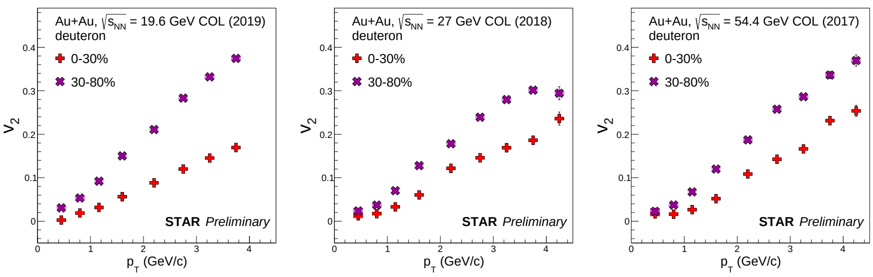

Fig. 3. $v_2(p_T)$ of d measured in 0-30% and 30-80% centrality intervals in Au+Au collisions at $\sqrt{s_{NN}}$ = 19.6, 27, and 54.4 GeV. Vertical lines and shaded bands at each marker represent statistical and systematic uncertainties, respectively.

5. Mass number scaling

According to the coalescence model, assuming that protons and neutrons behave in the same way, for a light nuclei N with mass number A, we expect[5,13]

$$v_{2,N}(p_T) \approx A v_{2,p}(p_T/A), \tag{3}$$

where $v_{2,p}$ is elliptic flow of protons. This is referred to as mass number scaling. Figure 4 shows the comparison of v_2/A of d, t, and ^{3}He as a function of p_T/A (where A is the mass number of the nuclei) with v_2/A of proton (where $A = 1$). v_2 of proton has been fitted with a third-order polynomial. The bottom panel in each plot shows the ratio between v_2/A of light nuclei and the fit to proton v_2. It is observed that v_2 of light nuclei deviates from mass number scaling by 20-30%. Although simple mass number scaling does not seem to hold for the studied collision energies, a more advanced coalescence model taking into account the phase-space distribution of the constituent protons and neutrons, might describe the elliptic flow of light nuclei better. Therefore, additional model studies are required to conclude whether the coalescence model is the dominant production mechanism of light nuclei.

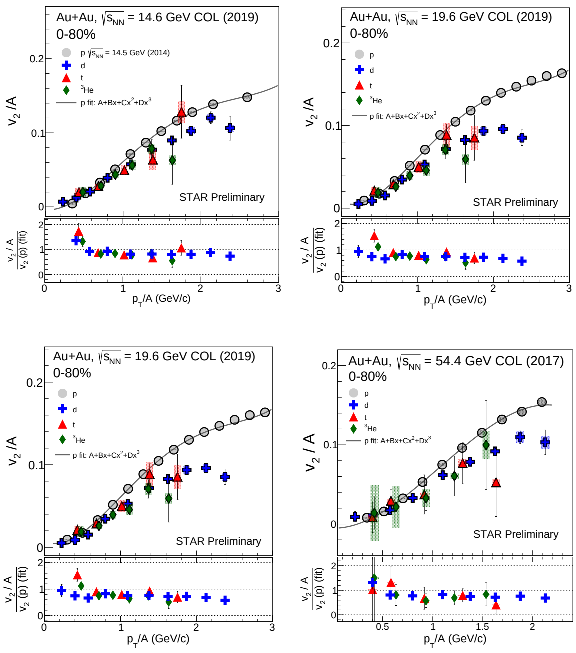

Fig. 4. Mass number scaling of v_2 of p, d, t, and ^{3}He as a function of p_T/A in minimum bias Au+Au collisions at $\sqrt{s_{NN}}$ = 14.6, 19.6, 27, and 54.4 GeV. Gray solid lines correspond to third order polynomial fits to v_2 of p. Bottom panel in each plot shows the ratios of $[v_2/A]$/fit for d, t, and ^{3}He for each collision energy. Vertical lines and shaded bands at each marker represent statistical and systematic uncertainties, respectively.

6. Summary

In summary, we have reported v_2 of p, d, t, and ^{3}He in Au+Au collisions at $\sqrt{s_{NN}}$ = 14.6, 19.6, 27, and 54.4 GeV. A monotonic rise of light nuclei v_2 with p_T is observed for all light nuclei species and studied energies. Mass ordering is observed at low p_T in $1-2$ GeV/c range. v_2 of d is observed to show a strong centrality dependence being higher for peripheral collisions compared to central collisions. This behaviour can be attributed to the fact that peripheral collisions have higher spatial anisotropy compared to the central collisions. In addition, it is also observed that v_2 of light nuclei deviates from mass number scaling by 20-30%.

References

1. D. Oliinychenko, *Nucl. Phys. A* **1005**, 121754 (2021).
2. J. I. Kapusta, *Phys. Rev. C* **21**, 1301 (1980).
3. A. Andronic *et al.*, *Nature* **561**, 7723, 321-330 (2018).
4. S. T. Butler *et al.*, *Phys. Rev.* , **129**, 836 (1963).
5. T. Z. Yan *et al.*, *Phys. Lett. B*, **638**, 50-54 (2006).
6. K.H. Ackermann et al. (STAR Collaboration), *Nucl. Instrum. Meth. A*, **499** 624-632 (2003).
7. W.J. Llope, *Nucl. Instrum. Meth. B* **241** 306-310, (2005).
8. C. Yang, *J. Phys.: Conf. Ser.* **779**, 012082 (2017).
9. H. Bichsel, *Nucl. Instrum. Methods Phys. Res., Sect. A* **562**, 154 (2006).
10. W. J. Llope *et al.*, *Nucl. Instrum. Methods Phys. Res.*, **759**, 23 (2014).
11. S.A. Voloshin *et al.*, arXiv:0809.2949 [nucl-ex].
12. A. M. Poskanzer *et al.*, *Phys. Rev. C* **58**, 1671 (1998).
13. L. Adamczyk *et al.* (STAR Collaboration), *Phys. Rev. C* **94**, 034908 (2016).